and effective drugs in selectively targeting cancerous cells. In this study, new substituted aminobenzenesulfonamide derivatives were synthesized and subsequently tested for *in vitro* cytotoxicity activities using the cytotoxity MTT assay technique. The structures presented herein bear sulfonamide moieties connected via propanamide linkages to morpholino- and thiomorpholino-heterocycles and were examined for anticancer activities against several cancer lines and were compared to normal non-cancerous cell lines.

Results And Discussion

Chemistry

Scheme I illustrates the synthesis of two 2-bromo N^4-substituted benzenesulfonamides **3**,**4** followed by subsequent derivatization to the target substituted morpholino-, thiomorpholino- and piperazine aminobenzenesulfonamides derivatives **5-8**. 4-Aminobenzenesulfonamide **1** and 4-(2-aminoethyl) benzenesulfonamide **2** were reacted with 2-bromopropionyl bromide, separately, in pyridine solvent to give bromo substituted amides as the key intermediates **3** and **4**, respectively. These were then treated with the morpholino-, thiomorpholino- and 1-ethylpiperazine secondary amines in dry THF, in separate reactions, to obtain desired derivatives **5-8**, as white solid products in 70-80% yields.

The characterizations of the target N^4-substituted aminobenzenesulfonamide derivatives **5-8** were carried out using FT-IR, UV-Vis, ^{1}H and ^{13}C NMR, LC-MS-MS and elemental analyses and the respective data are given in the experimental section. The spectral bands and NMR data of synthesized compounds were in accordance with the structures proposed.

Cytotoxic Activity

Cell cultures

Cytotoxic assessments of the newly synthesized N^4-substituted aminobenzenesulfonamides derivatives **5-8** were carried using the *in vitro* MTT assay technique against six cancer cell lines, including human prostate cancer (PC-3 and DU-145), human colorectal adenocarcinoma (HT-29), cervix carcinoma (HeLa), colorectal adenocarcinoma (DLD-1) and endometrial carcinoma (ECC-1), and were compared for their effects in normal non-cancerous human prostate epithelium (PNT-1A) and embryonic kidney (HEK-293). Table I provides the IC_{50} values of synthesized compounds. Cells were subjected to propagation using DMEM-F12 and RPMI-1640 media, and media supplements foetal bovine serum (10 %), L-glutamine (2mM), penicillin (100 U/mL) and streptomycin (100 mg/mL) in a humidified atmosphere (5% CO_2) were provided at 37 °C. The cell cultures were harvested using 0.25% trypsin (Sigma), upon reaching 70-80% confluence, as recommended by ATCC.

MTT-based cytotoxicity assay

Cytotoxic activities were determined by the colorimetric 3-(4, 5-dimethylthiazol-2-yl)-2, 5-diphenyl tetrazolium bromide (MTT) assay, where the reduction of MTT by mitochondrial dehydrogenase of viable cells leads to the formation of purple formazan product, spectrophotometrically detected by UV-Vis measurements[13]. MTT

Scheme I — Reaction diagram for the synthesis of N^4-substituted aminobenzenesulfonamides **5-8**

Table I — Measured IC_{50} values of precursors **1** and **2**, and N^4-substituted benzenesulfonamides **5-8** against tumor and normal cell lines

Compd	IC_{50} (μM)[a,b]							
	Cancer Cell						Normal Cell	
	PC-3	DU-145	HT-29	HeLa	DLD-1	ECC-1	PNT1-A	HEK-293
1	>250	>250	>250	>250	36.19	23.63	>250	>250
2	>250	>250	>250	111.00	>250	>250	>250	>250
5	>250	>250	231.00	>250	>250	>250	>250	>250
6	>250	116.00	204.00	>250	>250	>250	139.00	42.00
7	>250	>250	>250	>250	26.12	47.35	>250	>250
8	57.67	>250	>250	180.12	73.12	>250	>250	>250
5-FU	45.20	37.40	23.40	19.20	50.90	30.20	142.10	65.30

[a]Mean IC_{50} value of three independent readings.

[b]IC_{50} values determined at 48 h treatment period.

colorimetric assays were carried out as described in our previous work[9]. Briefly, 96 microwell plates were used, and were seeded (5.0 x 10^4 cells/well) and incubated at 37 °C for 24 h, prior to the addition of the test compounds. The cells were treated with the test compounds of various concentrations (1, 5, 10, 25, 50, 100 and 200 μM) and incubated for a further 48 h at 37 °C. Upon medium removal, cells were incubated with 100 μL MTT solution (5 mg/mL) at 37 °C for 4 h. Upon the removal of the MTT solution, followed by dissolution with 100 μL DMSO, the optical absorbances were measured at 570 nm. Cytotoxicities were determined with reference to the negative controls and expressed as the mean percentage increase relative to unexposed controls; the results were mean ± standard deviation of triplicate readings. Control values were set as 100% cytotoxicity, and where necessary cytoxicity data were fitted to sigmoidal curves and a four-parameter logistic model for calculating IC_{50} values; IC_{50} was the concentration required to inhibit 50% cancer cell growth. The positive control used was 5-fluorouracil (5-FU). Results are given in Table I.

The newly synthesized target compounds **5-8** were tested for cytotoxic activities, where the data were expressed as IC_{50} and are provided in Table I. The target compounds **5-8** revealed cytotoxic effects against various cells studied, with no remarkable cytotoxicity and only minimal effects on normal non-cancerous cells.

Compound **5** of morpholino- sulfamoylphenyl propanamide structure exhibited weak cytotoxicity against the HT-29 cell type with IC_{50} value 231.00 μM. Compound **5** exhibited weak cytotoxicity against the HT-29 cell type with no cytotoxicity on normal cells. Compound **6** of morpholino (sulfamoylphenyl) ethylpropanamide structure, with one carbon extension of the main amide chain, had cytotoxic effect on DU-145 and HT-29, however was active against normal cells. This slight chain elongation can result an increase in lipophilic character of the compound. It was observed that compound **7** had cytotoxic effects on DLD-1 and ECC-1 cell type whilst no cytotoxicity on normal cells was observed. The commonly used chemotherapeutic agent 5-fluorouracil (5-FU) served as the positive control for evaluating the chemotherapeutical effects. Cytotoxic effect of **7** on DLD-1 cell type can be considered remarkable due to lower IC_{50} values compared with compound **1** and 5-FU. Compound **8** was considerably active against PC-3 and DLD-1 cell types and moderately so for the HeLa cell type, while unaffecting normal cells.

Lipophilicity and electronic properties

Physicochemical properties of newly synthesized substituted aminobenzenesulfonamide derivatives were carried to assertain correlations of the biological activities of synthesized compounds with physicochemical descriptors[20-22]. Several molecular descriptors of the synthesized substituted aminobenzenesulfonamide derivatives are given in Table II.

Lipophilicity or partition coefficient may be described as logP and can provide important information regarding the passage of compounds through membranes for pharmacological effects. Log P was positive for lipophilic and negative for hydrophilic samples.

Table II shows the synthesized propionamide structures **5**, **7** and **8** had the greatest lipophilicities. The precursor compound sulfanilamide **1** had greater

Table II — Various physicochemical descriptors for precursors compounds **1** and **2**, and N^4-substituted benzenesulfonamides **5**-**8**

Compd	logP	MW	MV (Å^3)	MR (Å^3)	HOMO (eV)	LUMO (eV)	ΔE (eV)	Total Energy (eV)	Dipole Moment, μ (D)
1	-1.98	172.20	480.62	47.76	-9.305	-0.658	8.647	-1931.71	6.554
2	-1.20	200.26	599.97	56.68	-9.797	-0.863	8.934	-2230.52	5.018
5	-2.09	313.37	877.04	84.20	-9.580	-0.776	8.804	-3680.54	4.957
6	-1.31	341.43	960.45	93.12	-9.602	-0.888	8.714	-3979.54	6.101
7	-1.65	329.43	896.00	90.37	-9.106	-0.906	8.200	-3572.90	6.901
8	-1.60	340.44	980.87	95.92	-8.984	-1.048	7.936	-3863.58	2.993

lipophilicity than the synthesized compounds **6**-**8**. Interestingly, compounds **7**, **8** and precursor compound **1** gave the greatest cytotoxic effects on DLD-1, ECC-1 and PC-3 cell types, where compound **7** had the greatest cytotoxic effect (IC_{50} 26.12 μM on DLD-1 and 47.35 μM on ECC-1), followed by precursor compound **1** (IC_{50} 36.19 μM on DLD-1 and 23.63 μM on ECC-1), and finally compound **8** (IC_{50} 73.12 μM on DLD-1 and 57.67 μM on PC-3). While compound **7** stems from 4-aminobenzenesulfonamide, amino substituted with the three-atom chain propionamide structure, having with a thiomorpholino- group at position-2 of the amino chain, compound **8** of similar structure, also with the three-atom propionamide chain, having a piperazine, para-substituted with an ethyl group (N^4-ethyl group substitution). The precursor compound **1** was 4-aminobenzenesulfonamide compound, with unsubstituted amino group at the para position. Chain elongation of the para amino group gives the second precursor compound **2** being 4-(2-aminoethyl)benzenesulfonamide. In regard to the synthesized compounds, it seemed that electronegativity of the para- oxa, sulfa and aza atoms played a dominating role on cancer cell cytotoxicity. Structures **5** and **6**, both bear a para- oxa atom in its morpholino moiety, and this oxa atom has greater electronegativity than the sulfa and aza atoms, existing in the corresponding positions of the thiomorpholino- and piperazine structures **7** and **8**, respectively. However, the aza atom is a much softer Lewis base than an oxa atom as present in structures **5** and **6**, thus leading to better electron donating properties, hence better hydrogen bond acceptors in the interactions leading to possible cancer cell death. Thus, a combination of electronegativity and availability of the electrons of these heteroatoms appeared to have an effect on cancer cell cytotoxicity. In regard to the precursor compound **1**, this structure had high cancer cell cytotoxicity against DLD-1 and ECC-1 cell types, and further amino substitutions with an additional three-atom propionamide chain bearing thiomorpholino- and piperazine moieties as for structures **7** and **8**, may preserve or improve cancer cell toxicities. While the aza atom as in the piperazine moiety of structure **8** has greater electronegativiy than the sulfa atom, as in the thiomorpholino- moiety of structure **7**, this was outbalanced by the aza atom of piperazine structure **8** as it was not free, but bound to an ethyl group, thus reducing the effective electronegativity and hydrogen bond accepting ability of aza atom of structure **8**. Therefore, as a result of this N^4-ethyl group substitution, the observed overall cytotoxic effect of structure **8** on cell types DLD-1 and PC-3, though high compared to the other compounds **2**, **5** and **6**, was less than that observed for structure **1** and more so for structure **7**.

Further, the dipole effects were the greatest for synthesized compounds **6**, and **7** and precursor compound **1** of dipole values (μ) greater than 6.000 D, being 6.101, 6.901 and 6.554 D, respectively. Here it can be noted that while high lipophilicity is required for cancer cell attack, the moderately lipophilic compound **6** has a high dipole value. Thus, in regard to compound **6**, it can be noted that moderate lipophicity and overwhelming dipole characteristics may have synergetics results on cell toxicity, allowing for the unfavorable interactions against normal human cell types PNT1-A, and more so on HEK-293, and weak cytotoxic effects on cancer cell types DU-145 and HT-29. This was not observed for compounds **1** and **7**, as though both have great dipoles, both are also highly lipophilic. In contrast, compound **5** is highly lipophilic but has a poor dipole value. Thus, compound **5** had no remarkable cancer cell toxicity effects, just minimal effects on cancer cell type HT-29.

The molecular volumes (MV), molecular refractivities (MR) and molecular weights (MW) of

the synthesized compounds were greater than the precursor compounds **1** and **2** and were in the order **5**>**6**>**7**>**8**, where among these, structure **8** had the greatest values.

Energetics and electronic dipole studies

The frontier features HOMO and LUMO of the structures synthesized were examined as qualitative details regarding the molecular structures may be retrieved. Structures of the synthesized compounds were optimized prior to data retrieval.

Derivative **5** revealed that 58 of 103 occupied molecular orbitals, with the HOMO and LUMO orbitals computed as -9.580 and -0.776 eV, respectively, with energy gap (ΔE) 8.804 eV. Derivative **6** had 64 of 115 occupied molecular orbitals, with HOMO and LUMO orbitals at -9.602 and -0.888 eV, respectively, with ΔE 8.714 eV. Derivative **7** revealed 58 of 103, with HOMO and LUMO orbitals at -9.106 and -0.906, respectively, with ΔE 8.200 eV. Derivative **8** gave 64 of 116 molecular orbitals occupied, with HOMO and LUMO orbitals at -8.984 and -1.048 eV, respectively, with ΔE 7.936 eV. Table II showed that the ΔE of HOMO-LUMO for the synthesized derivatives **7** and **8** were the lowest values. These differences may have some role on observed cytotoxic effects, where the observed cytotoxic effetcs of derivatives **7** and **8** were somewhat similar. Derivative **5** had a high dipole moment, possibly a favoured condition for cancer cell electrostatic interactions and eventual breakdown, however, this was surpassed by its low lipophilic nature, as shown in Table II, and hence the observed interactions against normal human cell types PNT1-A and HEK-293, and only weak cytotoxic effects on cancer cell types DU-145 and HT-29.

Fourier Transform Infrared spectroscopy (FT-IR) measurements

FT-IR spectra of the newly synthesized benzenesulfonamide derivatives **5-8** were obtained using U-ATR at range 4000-400 cm^{-1} and were compared those of the starting compounds to obtain interesting information for spectroscopic characterization of the novel compounds. Synthesized compounds **5-8** showed characteristic vibrations at ranges of 3340-3250 cm^{-1} for -NH_2 sulfonamide, 3220-3180 cm^{-1} for N-H amide, 1695-1630 cm^{-1} for C=O amide, 1340-1160 cm^{-1} for S=O sulfonamide as given in the experimental section. These confirmed formation of novel N^4-substituted aminobenzenesulfonamides **5-8** (Figure 1).

UV-Vis data analyses

Spectrophotometric grade DMF was used for collecting the electronic spectra of precursors **1** and **2**, 2-bromo N^4-substituted benzenesulfonamides **3** and **4** and N^4-substituted benzenesulfonamides **5-8**, and are presented in Figure 2.

Precursor **1** gave a strong absorption at 276 nm and a weak band at 306 nm; this was consistent with the literature values[23-25]. The 276 nm absorption was designated as the benzenoid ring π-π* transition. The 306 nm absorption shows n-π* transitions arising from non-bonding electrons of the N or S atoms of compound **1**. These two peaks observed for precursor **1** illustrates the presence of two transition types, the first being strong and the most probable occurrence,

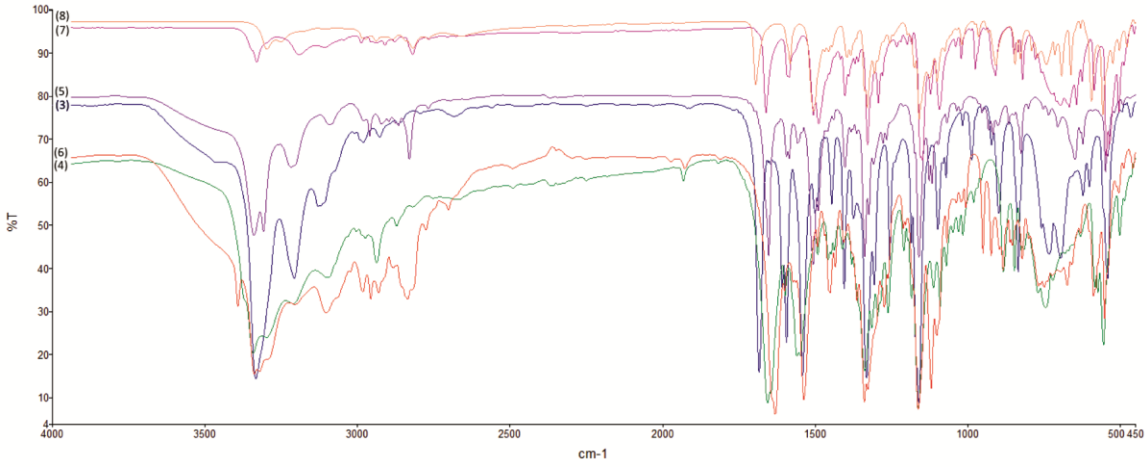

Figure 1 — FT-IR spectra of precursors **1** and **2**, 2-bromo N^4-substituted benzenesulfonamides **3** and **4** and N^4-substituted benzenesulfonamides **5-8**

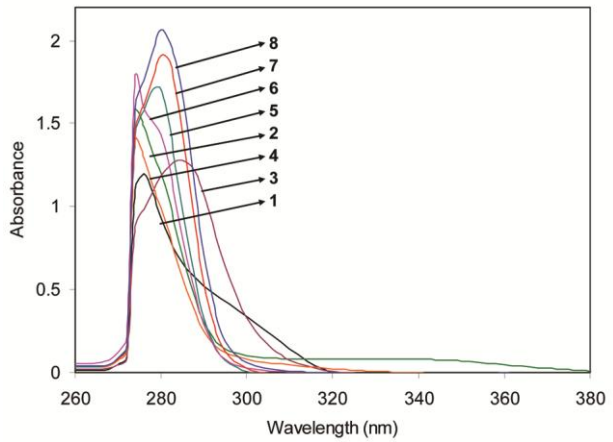

Figure 2 — UV-Vis spectra of precursors **1** and **2** and 2-bromo N^4-substituted benzenesulfonamides **3** and **4** and N^4-substituted benzenesulfonamides **5**-**8**

and the second being much weak and occurring with lower chance. Figure 2 showed all the synthesized compounds **3**-**8** as having different absorption spectra due to their differing observed λ_{max}, particularly for intermediate compound **3**. Further, intermediate compound **3** had an intense absorption at 284 nm and a shoulder peak at 298 nm. Compound **3** had a main absorption being much broader than that of compound **1**, shifting slightly to a higher wavelength (from 276 nm to 284 nm).

Precursor **2** leads to its intermediate compound **4** and upon reaction, as detailed out in the experimental section, provides derivative **6**. The absorption 274 nm can be attributed to the π-π* transitions for compounds **2**, **4** and **6**. The main absorption peaks for these compounds were sharper and more attenuated than that of precursor **1**, shifting to lower wavelength (from 276 nm to 274 nm). The weak band noted at 306 nm for precursor **1** was relatively poor in precursor **2**, and its respective intermediate **4** and its related derivative **6**. This indicated that the n-π* transitions in compounds **2**, **4** and **6** were less distinct, and the the π-π* transitions for compounds **2**, **4** and **6** were the dominating transitions. The π-π* transition peak intensities for compounds **2**, **4** and **6** were greater than precursor **1**. Structures bearing rich electronic structures may notably increase maxima absorption intensities. Further, chain elongation, such as an ethyl chain, led to higher absorption maxima intensities, and maxima absorption shifts as for compounds **2**, **4** and **6** compared to the absorption maximum wavelength of precursor **1**. The 280 nm absorption was designated as the π-π* transitions for derivatives **5**, **7** and **8**. The main absorptions for

Table III — UV-Vis data for precursors **1** and **2**, 2-bromo N^4-substituted benzenesulfonamides **3** and **4** and N^4-substituted benzenesulfonamides **5**-**8**

Compd	ε (L mol^{-1} cm^{-1})	λ_{max} Abs (nm)	In Abs
1	8.54x10^4	276	1.196
2	11.28x10^4	274	1.579
3	9.11x10^4	284	1.276
4	10.02x10^4	274	1.403
5	12.17x10^4	278	1.704
6	12.70x10^4	274	1.778
7	13.61x10^4	280	1.906
8	14.75x10^4	280	2.065

λ_{max} Abs: maximum absorption wavelength, In Abs: maximum absorption intensity, ε: molar absorptivity coefficient, sample concentrations: 1.4x10^{-5} mol/L

derivatives **5**, **7** and **8** were narrower than that of precursor **1**, shifting to higher wavelengths (from 276 nm to 280 nm). The weak band observed at 306 nm for precursor **1** was indistinguishable for derivatives **5**, **7** and **8**, hence the π-π* transitions for derivatives **5**, **7** and **8** were the dominating transitions. Derivatives **5**, **7** and **8**, bearing larger cyclic structural units, led to high π-π* transition peak intensities, compared to that of precursor **1**. This may be due to these derivatives being structurally more cyclic and capable of donating π electrons, and can result in increased absorption maxima intensities. Among the derivatives synthesized, derivative **8** was observed as having the greatest absorption maximum intensity.

UV-Vis data for precursors **1** and **2** and 2-bromo N^4-substituted benzenesulfonamides **3** and **4** and N^4-substituted benzenesulfonamides **5**-**8** are given in Table III. The values of molar absorptivity coefficients for compounds **2**-**8** were greater than that of precursor **1**. Notable increases in the molar absorption capacities were observed for these compounds compared to precursor **1**. A plausible explanation for this may be that these structures are much more electron rich than precursor **1**. Among the derivatives **5**-**8**, derivative **8** displayed the greatest molar absorptivity coefficient value, where the differences in the values of molar absorptivity coefficients may be due to the structural differences, and respective atomic contributions to electronic energy levels of the compounds.

^{1}H and ^{13}C NMR spectroscopic analyses

NMR spectra data of the newly synthesized benzenesulfonamide derivatives **5**-**8** are given in the experimental section. The NMR spectra of derivatives

5 and **7** are provided as representative examples, and are given in Figure 3, Figure 4, Figure 5 and Figure 6. The ^{1}H NMR spectra of derivatives **5**-**8** showed aliphatic protons in range δ 0.96-3.73 ppm, and aromatic protons in range δ 7.35-7.84 ppm, and are consistent with the literature[9,26]. Further, derivatives **5**-**8** exhibited singlets at 7.81-10.10 ppm, these being attributed to the amide proton (-CONH) and at 7.23-7.28 ppm, attributed to the sulfonamide protons (-SO_2NH_2). Doublet peaks were seen for the CH_3- and aromatic methylene proton (Ar-H) groups, both of which neighboured single protons. Multiplet peaks were noted, and assigned to the aromatic protons (Ar-H) of benzenesulfonamide ring for all the derivatives and methylene (-CH_2-) protons of morpholine, thiomorpholine and 1-ethly piperazine rings for derivatives **5**-**8.**

The ^{13}C NMR spectra of derivatives **5**-**8** gave aliphatic methyl carbons at δ 11.37-13.47 ppm, particularly derivative **8** gave an extra methyl carbon at δ 12.49 due to 1-ethyl piperazine moiety and aromatic carbons at δ 119.40-144.07 ppm being

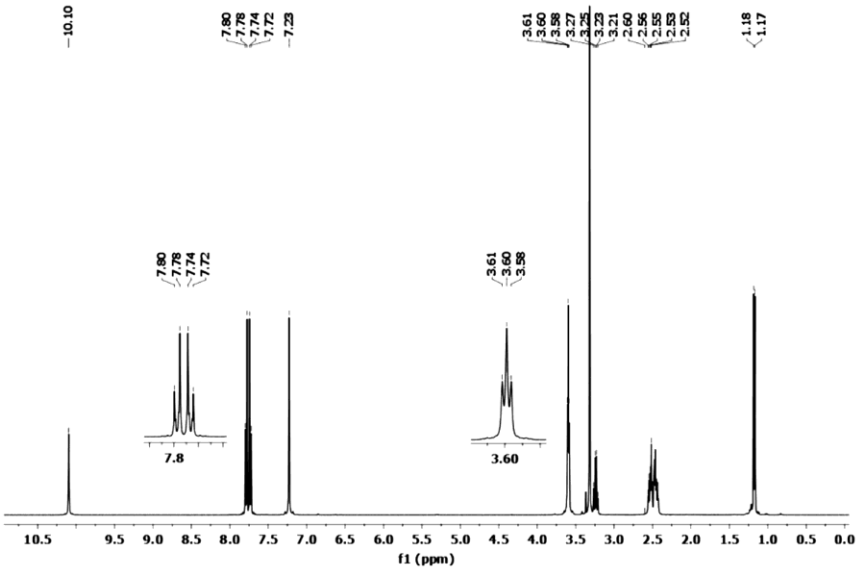

Figure 3 — ^{1}H NMR spectrum of derivative **5**

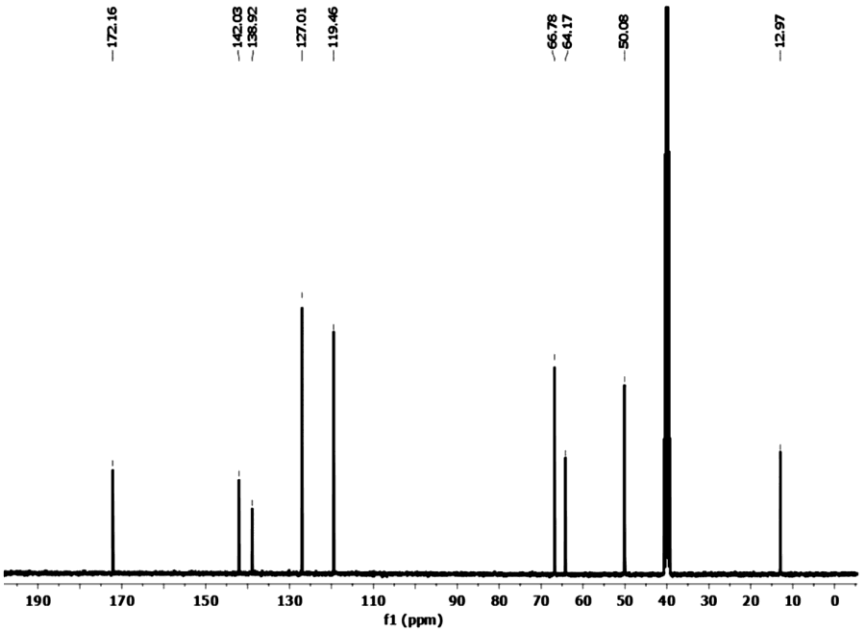

Figure 4 — ^{13}C NMR spectrum of derivative **5**

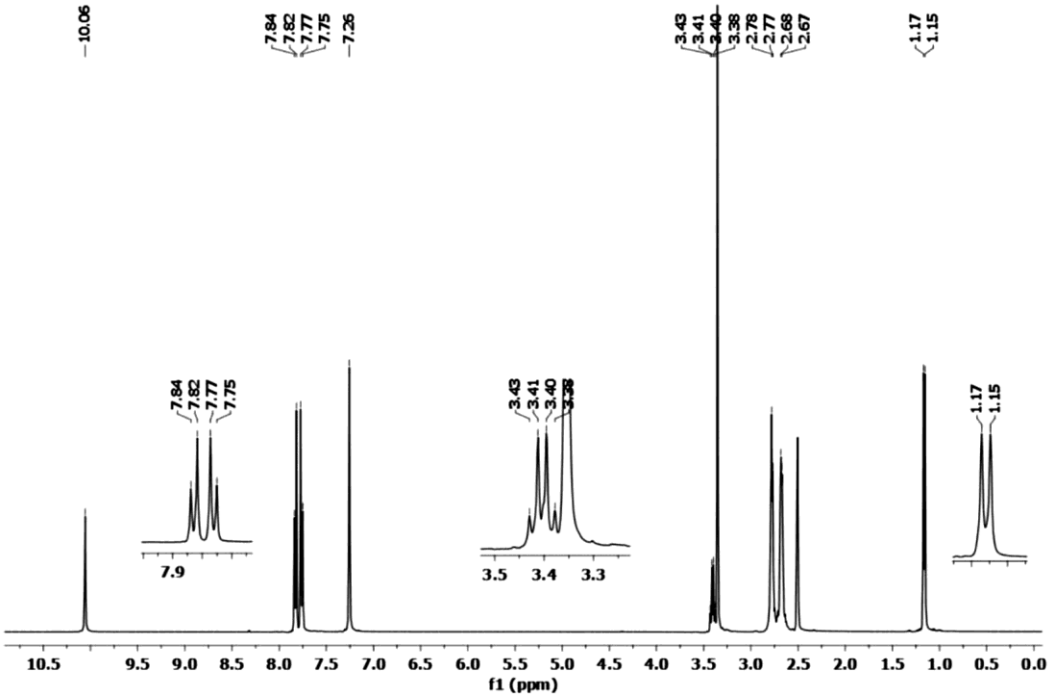

Figure 5 — ^{1}H NMR spectrum of derivative **7**

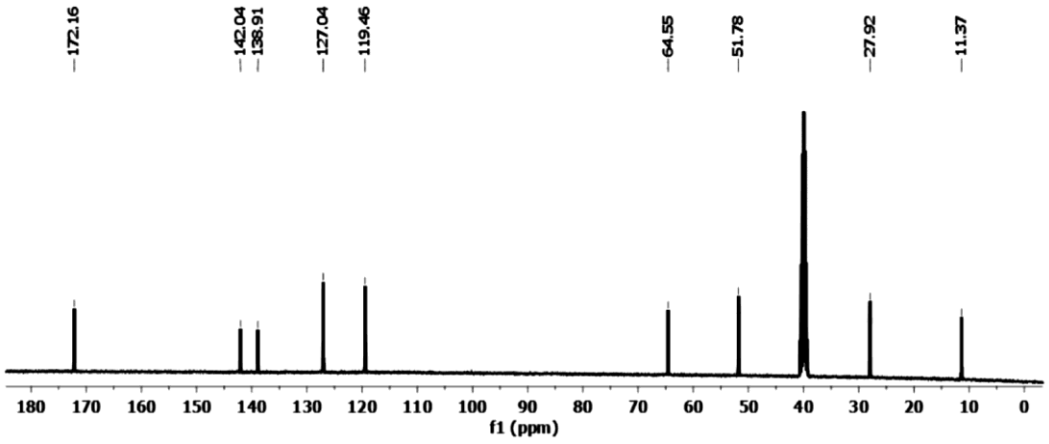

Figure 6 — ^{13}C NMR spectrum of derivative **7**

consistent with the literature[9,26]. Methylene ring carbons were observed in the region 27.92-64.17 ppm, where shift values depended on the ring size and type. The amide carbon (-CONH) was observed in the region 172.16-172.60 ppm. Several aromatic carbons had the exact same NMR signal, due to the symmetry of the molecular structures[9,26].

Mass spectral (LC-MS-MS) evaluations

The molecular mass data of the newly synthesized benzenesulfonamide derivatives **5**-**8** were collected and spectral analysis revealed the formation of the target compounds. The mass spectra of derivatives **5** and **7** are given as representative examples, and are provided in Figure 7 and Figure 8, respectively. Data collected support the formation of target derivatives which were detected as single sharp peaks, indicative of the $[M+H]^+$ ions.

Fluorescence spectroscopy measurements

Fluorescence spectra for precursors **1** and **2** and compounds **3**-**8**, with excitation at 264 nm, were evaluated. Upon irradiation by UV light, precursors **1** and **2** and compounds **3**-**8** provided strong fluorescence emissions. The fluorescence spectra for precursors **1** and **2**, 2-bromo N^4-substituted

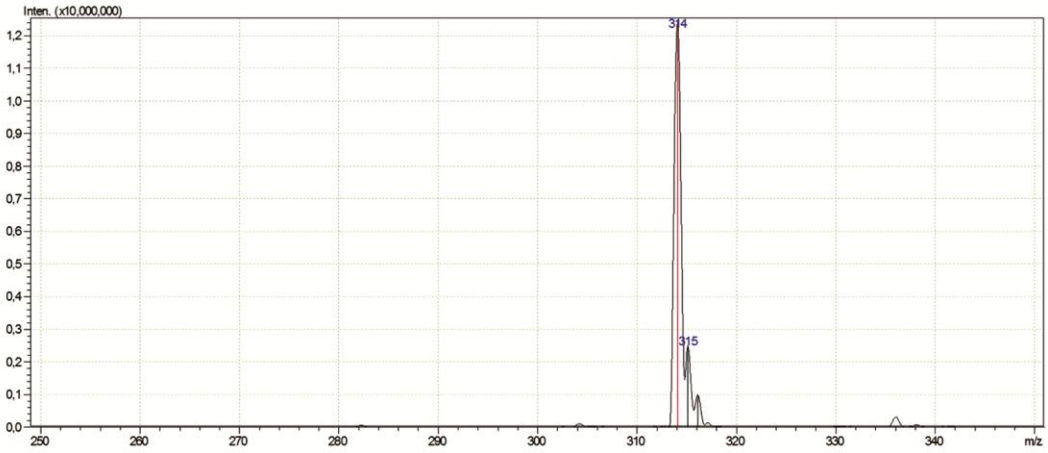

Figure 7 — Mass spectrum of derivative **5**

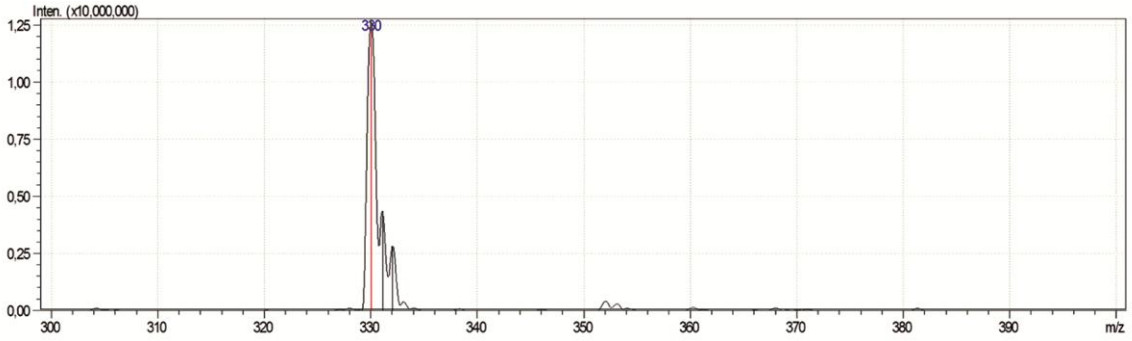

Figure 8 — Mass spectrum of derivative **7**

benzenesulfonamides **3** and **4** and N^4-substituted benzenesulfonamides **5**-**8** are given in Figure 9.

The maximum luminescent intensity for precursor **1** was 348 nm, having a full width at half maximum (FWHM) of 48 nm. Further, precursor **1** provided a quantum yield of 27 %, and excited-state lifetime of 2.57 ns. The maximum luminescent intensity for derivative **8** was 391 nm, with its respective FWHM being 106 nm, and a quantum yield of 37 % and 3.48 ns excited-state lifetime. Increasing electron donating groups at ring para-positions caused increases in the main peak intensities, as observed for compounds **2** and **4**-**8**, shifting to higher emission wavelengths. Extended molecular structures bearing high π-electron delocalizations or the existence of electron rich cyclic molecules result in high quantum yields and increases in fluorescence emission intensities. Electron rich structures improve electron delocalizations and/or energy transfers from derivative excited states and leds to decreases in the non-radiated transitions of the derivatives and eventual increases of fluorescence emissions. Further, attachments of electron withdrawing groups at ring para- positions as for

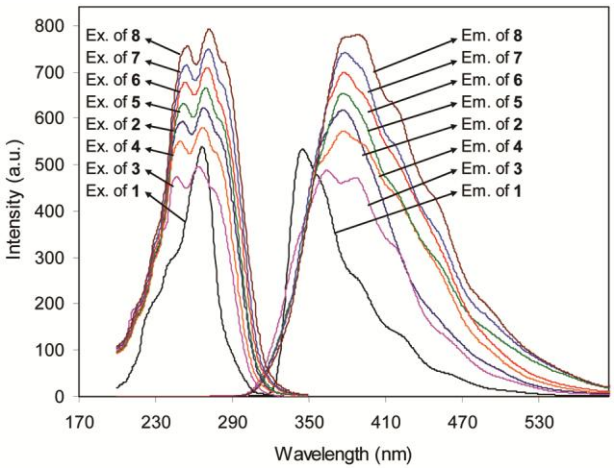

Figure 9 — Fluorescence spectra for precursors **1** and **2**, 2-bromo N^4-substituted benzenesulfonamides **3** and **4** and N^4-substituted benzenesulfonamides **5**-**8** in DMF, with excitation at 264 nm

compound **3** results in main peak intensity decreases, shifting to lower emission wavelengths as reported earlier[9]. These electron withdrawing groups pull electrons and reduce the possibility of emissions from cyclic derivative excited states. The fluorescence spectral data for precursors **1** and **2**, 2-bromo

Table IV — Fluorescence data for precursors **1** and **2**, 2-bromo N^4-substituted benzenesulfonamides **3** and **4** and N^4-substituted benzenesulfonamides **5-8**

Compd	λ_{max} Ex (nm)	In Ex	λ_{max} Em (nm)	In Em	ϕ_f (%)	τ_f (ns)
1	268 (225;243;259)	533	348 (362;391;427)	526	27	2.57
2	270 (216;228;253;283)	617	379 (344;359;404;451)	608	31	2.90
3	266 (214;225;249;279)	491	366 (342;389;421;461)	485	26	2.40
4	269 (215;227;252;281)	575	378 (356;396;422;453)	567	29	2.73
5	271 (217;229;254;284)	659	380 (360;397;423;454)	649	33	3.05
6	272 (217;230;255;285)	701	381 (361;398;424;456)	690	34	3.21
7	273 (218;231;256;286)	743	383 (363;396;423;457)	731	36	3.34
8	274 (218;231;257;287)	785	391 (378;423;453;497)	772	37	3.48

λ_{max} Ex: maximum excitation wavelength; In Ex: maximum excitation intensity;
λ_{max} Em: maximum emission wavelength; In Em: maximum emission intensity;
ϕ_f : quantum yield; τ_f : excited-state lifetime.

N^4-substituted benzenesulfonamides **3** and **4** and N^4-substituted benzenesulfonamides **5-8** are given in Table IV.

Experimental Section

Materials and chemicals

Chemicals, solvents and reagents were purchased from commercial suppliers and were used without further purification unless indicated in the procedures.

Instrumentation and measurements

A LECO CHNS-932 Elemental Analyser was used for elemental analysis detections. FT-IR spectra were collected using a Perkin Elmer Spectrum Two FT-IR Spectrometer. Electronic absorption spectra were measured using a Perkin Elmer Lambda 25 UV-Vis Spectrophotometer. A Perkin Elmer LS55 Spectrofluorophotometer was used for the fluorescence measurements using quartz sample cells of 1 cm optical path and sample concentrations in DMF being 1.0×10^{-5} $molL^{-1}$, and the applied excitation wavelength 264 nm. Photoluminescence quantum yield measurements were taken using the standard 9,10-diphenylantracene[16-18]. An Agilent-VNMRS-400 Spectrometer was used for NMR data (^{1}H NMR 400 MHz, ^{13}C NMR 100 MHz) collections, utilizing DMSO-d_6 as the solvent and TMS as the internal standard. An Electrothermal 9100 melting point apparatus was used for the melting point readings. Mass spectral data were collected using a Shimadzu LCMS 8040 Model Spectrometer. Purity assessments and reaction progress were followed using chromatography plates (Merck Silica Gel 60 F_{254}).

In vitro Cytotoxic Activity

Cell culture preparation

Cells studied were provided by the American Type Culture Collection (ATCC, Manassas, Virginia). Cell types investigated were cancerous human prostate (PC-3 and DU-145), human colorectal adenocarcinoma (HT-29), cervix carcinoma (HeLa), colorectal adenocarcinoma (DLD-1), endometrial carcinoma (ECC-1) cell types, and normal prostate epithelium PNT-1A and embryonic kidney (HEK-293). Cells were subjected to propagation processes, with supplements of foetal bovine serum, L-glutamine, penicillin and streptomycin in a 37 °C humidified atmosphere as described previously[9]. Upon reaching 70–80% confluence, the cells were harvested as recommended by ATCC.

Cytotoxicity and IC_{50} determination

The reduction of (3-(4,5-dimethylthiazol-2-yl)-2,5-diphenyltetrazolium bromide) (MTT) detected spectrophotometrically as blue formazan production, allowed for cytotoxicity evaluation[13]. Using a literature procedure, 96 well plates was used for the MTT colorimetric assays, seeded at concentration 5.0×10^4 cells/well with 37 °C incubations for 24 h[9]. The test concentrations used were 1, 5, 10, 25, 50, 100 and

200 μM, with data collections carried out triplicate readings and negative controls as the reference.

Physicochemical properties studies

Some parameters were calculated in order to establish the relationship between the evaluation of physicochemical properties and biological processes. Physiochemical descriptors were examined using HyperChem[19]. Molecular Mechanics Force Field (MM+) method was used for pre-optimizations and refinements by the semiempirical PM3 procedure.

General procedure for synnthesis of 2-bromo-*N*-(4-sulfamoylphenyl)propanamide 3 and 2-bromo-*N*-(4-sulfamoylphenethyl)propanamide, 4

A 10.00 mmol solution of 2-bromopropionyl bromide in 40 mL THF was slowly added to a 10.00 mmol solution of either 4-aminobenzenesulfonamide **1** or 4-(2-aminoethyl) benzenesulfonamide **2** and 15.00 mmol pyridine in 30 mL THF at 0°C. Upon warming to room temperature, the reaction was stirred for a further 22 h to give white solids **3** and **4**, respectively, as described in the literature method[9].

2-Bromo-*N*-(4-sulfamoylphenyl)propanamide, 3

Title compound **3** was a white solid (70%): m.p. 217-219 °C. FT-IR (U-ATR, cm^{-1}): 3333, 3207 (NH_2), 3129 (Amide-N-H), 3071 (Ar-C-H), 2927, 2980 (Aliph.-C-H), 1683 (Amide-C=O), 1331 (Asymmetric), 1160 (Symmetric) (S=O), 541 (C-Br); ^{1}H-NMR (DMSO-d_6, TMS, 400 MHz, δ ppm): 10.66 (1H, s, *H*-N-C=O), 7.71-7.77 (4H, m, *J*= 8 Hz, -Ar-H), 7.27 (2H, s, SO_2NH_2), 4.66-4.71 (1H, q, *J*= 8 Hz, Br-C*H*-), 1.72-1.74 (3H, d, *J*= 8 Hz, -CH_3); ^{13}C-NMR (DMSO-d_6, TMS, 100 MHz, δ ppm): 168.44 (C=O), 141.89 (Ar-C-NH-), 139.37 (Ar-C-SO_2NH_2), 127.22 (Arom.), 119.39 (Arom.), 44.56 (*C*H-Br), 21.64 (*C*H_3); LC-MS/MS Mass (*m/z*): 307.8 [M+H]; Calculated for $C_9H_{11}BrN_2O_3S$ (307.16 g/mol) (%): C, 35.19; H, 3.61; N, 9.12; S, 10.44. Found (%): C, 35.10; H, 3.67; N, 9.19; S, 10.35.

2-Bromo-*N*-(4-sulfamoylphenethyl)propanamide, 4

Title compound **4** was a white solid (70%): m.p. 159-161 °C. FT-IR (U-ATR, cm^{-1}): 3342, 3296 (NH_2), 3211 (Amide-N-H), 3095 (Ar-C-H), 3004, 2872 (Aliph.-C-H), 1655 (Amide-C=O), 1337 (Asymmetric), 1161 (Symmetric) (S=O), 554 (C-Br); ^{1}H-NMR (DMSO-d_6, TMS, 400 MHz, δ ppm): 8.33 (1H, s, *H*-N-C=O), 7.36-7.38 (2H, m, *J*= 8 Hz, -Ar-H), 7.70-7.72 (2H, m, *J*= 8 Hz, -Ar-H), 7.28 (2H, s, SO_2NH_2), 4.40-4.45 (1H, q, *J*= 8 Hz, Br-C*H*-), 3.27-3.32 (2H, m, N-CH_2); 2.76-2.79 (2H, d, *J*= 8 Hz, Ar-CH_2); 1.59-1.61 (3H, d, *J*= 8 Hz, -CH_3); ^{13}C-NMR (DMSO-d_6, TMS, 100 MHz, δ ppm): 169.02 (C=O), 143.56 (Ar-C-(CH_2)2-NH-), 142.26 (Ar-C-SO_2NH_2), 129.35 (Arom.), 125.79 (Arom.), 44.18 (*C*H-Br), 40.18 (CH_2-NH-), 34.51 (Ar-CH_2), 21.91 (*C*H_3); LC-MS/MS Mass (*m/z*): 336.2 [M+H]; Calculated for $C_{11}H_{15}BrN_2O_3S$ (335.22 g/mol) (%): C, 39.41; H, 4.51; N, 8.36; S, 9.57. Found (%): C, 39.33; H, 4.58; N, 8.47; S, 9.51.

General synthesis of N^4-substituted amino–benzenesulfonamides, 5-8

The syntheses of the title compounds were carried in a similar way to that described in the literature[9]. Briefly, mixtures of 1.5 equivalent samples of morpholine for the synthesis of **5**, thiomorpholine for **7** or 1-ethyl piperazine for **8** and a 1.0 equivalent sample of pyridine in 20.0 mL THF was slowly added to 10.00 mmol 2-bromo-*N*-(4-sulfamoylphenyl) propanamide **3** in 30 mL THF at 0 °C as separate reactions, over a period of 30 minutes. In the same manner, a mixture of a 1.5 equivalent sample of morpholine in 20.0 mL THF for the synthesis of **6** was slowly added to 10.00 mmol 2-bromo-*N*-(4-sulfamoylphenethyl)propanamide **4** in 30 mL THF at 0 °C, over a period of 30 minutes. Upon warming to room temperature, reactions were stirred at 40 °C for 48 h. All reactions were monitored by TLC (DCM/methanol). Recrystallizations were carried out for solid products using ethanol, and subsequently dried *in vacuo*.

2-Morpholino-*N*-(4-sulfamoylphenyl)propanamide, 5

Title compound **5** was a white solid (75%): m.p. 181-183 °C. FT-IR (U-ATR, cm^{-1}): 3339, 3308 (NH_2), 3219 (Amide-N-H), 3089 (Ar-C-H), 2960-2830 (Aliph.-C-H), 1652 (Amide-C=O), 1336 (Asymmetric), 1159 (Symmetric) (S=O); ^{1}H-NMR (DMSO-d_6, TMS, 400 MHz, δ ppm): 10.10 (1H, s, -CONH), 7.78-7.80 (2H, d, *J*=8 -Ar-H), 7.72-7.74 (2H, d, *J*=8, -Ar-H), 7.23 (2H, s, SO_2NH_2), 3.58-3.61 (4H, t, *J*=8, -CH_2-O-CH_2), 3.21-3.27 (1H, q, -N-C*H*-CH_3), 2.51-2.60 (4H, m, -CH_2-N-CH_2), 1.17-1.18 (3H, d, *J*=4 Hz -CH_3); ^{13}C-NMR (DMSO-d_6, TMS, 100 MHz, δ ppm): 172.16 (C=O), 142.03 (Ar-*C*-NH-), 138.92 (Ar-*C*-SO_2NH_2), 127.01 (Arom.), 119.46 (Arom.), 66.78 (CH_3-*C*H-N), 64.17 (*C*H_2-O-*C*H_2), 50.08 (*C*H_2-N-*C*H_2), 12.97 (*C*H_3); LC-MS/MS Mass

(*m/z*): 314.10 [M+H]; Calculated for $C_{13}H_{19}N_3O_4S$ (313.37 g/mol) (%): C, 49.83; H, 6.11; N, 13.41; S, 10.23. Found (%): C, 49.75; H, 6.14; N, 13.52; S, 10.19.

2-Morpholino-*N*-(4-sulfamoylphenethyl)propanamide, 6

Title compound **6** was a white solid (70%): m.p. 144-146 ˚C. FT-IR (U-ATR, cm^{-1}): 3338, 3320 (NH_2), 3210 (Amide-N-H), 3102 (Ar-C-H), 2982-2835 (Aliph.-C-H), 1630 (Amide-C=O), 1338 (Asymmetric), 1162 (Symmetric) (S=O); ^{1}H-NMR (DMSO-d_6, TMS, 400 MHz, δ ppm): 7.81 (1H, s, -CONH), 7.71-7.69 (2H, d, *J*=8, -Ar-H), 7.37-7.35 (2H, d, *J*=8 -Ar-H), 7.28 (2H, s, SO_2NH_2), 3.73-3.71 (2H, m, N-CH_2); 3.38-3.33 (1H, q, -N-C*H*-CH_3), 3.06-3.04 (2H, d, *J*= 8 Hz, Ar-CH_2); 2.83-2.78 (4H, t, *J*=8, -CH_2-O-CH_2), 2.31-2.22 (4H, m, -CH_2-N-CH_2), 1.02-1.00 (3H, d, *J*=4 Hz -CH_3); ^{13}C-NMR (DMSO-d_6, TMS, 100 MHz, δ ppm): 172.60(C=O), 144.07 (Ar-*C*-NH-), 142.47 (Ar-*C*-SO_2NH_2), 129.59 (Arom.), 126.02 (Arom.), 66.68 (CH_3-*C*H-N), 63.92 (*C*H_2-O-*C*H_2), 50.27 (*C*H_2-N-*C*H_2), 39.63 (CH_2-NH-), 35.11 (Ar-CH_2), 13.47 (*C*H_3); LC-MS/MS Mass (*m/z*): 342.10 [M+H]; Calculated. for $C_{15}H_{23}N_3O_4S$ (341.43 g/mol) (%): C, 52.77; H, 6.79; N, 12.31; S, 9.39. Found (%): C, 52.68; H, 6.85; N, 12.43; S, 9.31.

2-Thiomorpholino-*N*-(4-sulfamoylphenyl)propanamide, 7

Title compound **7** was a white solid (80%): m.p. 186-187°C. FT-IR (U-ATR, cm^{-1}): 3330, 3292 (NH_2), 3190 (Amide-N-H), 3105 (Ar-C-H), 2987-2819 (Aliph.-C-H), 1661 (Amide-C=O), 1328 (Asymmetric), 1148 (Symmetric) (S=O); ^{1}H-NMR (DMSO-d_6, TMS, 400 MHz, δ ppm): 10.06 (1H, s, -CONH), 7.82-7.84 (2H, d, *J*=8 -Ar-H), 7.75-7.77 (2H, d, *J*=8, -Ar-H), 7.26 (2H, s, SO_2NH_2), 2.79-2.77 (4H, t, *J*=8, -CH_2-N-CH_2), 3.38-3.43 (1H, q, -N-C*H*-CH_3), 2.67-2.69 (4H, m, -CH_2-S-CH_2), 1.15-1.17 (3H, d, *J*=4 Hz -CH_3); ^{13}C-NMR (DMSO-d_6, TMS, 100 MHz, δ ppm): 172.16 (C=O), 142.04 (Ar-*C*-NH-), 138.91 (Ar-*C*-SO_2NH_2), 127.04 (Arom.), 119.46 (Arom.), 64.55 (CH_3-*C*H-N), 51.78 (*C*H_2-N-*C*H_2), 27.92 (*C*H_2-S-*C*H_2), 11.37 (*C*H_3); LC-MS/MS Mass (*m/z*): 330.10 [M+H]; Calculated. for $C_{13}H_{19}N_3O_3S_2$ (329.44 g/mol) (%): C, 47.40; H, 5.81; N, 12.76; S, 19.47, Found (%): C, 47.32; H, 5.89; N, 12.88; S, 19.33.

2-(4-Ethylpiperazin-1-yl)-*N*-(4-sulfamoylphenyl)propanamide, 8

Title compound **8** was a white solid (70%): m.p. 221-222 ˚C. FT-IR (U-ATR, cm^{-1}): 3297, 3252 (NH_2), 3180 (Amide-N-H), 3043 (Ar-C-H), 2984-2790 (Aliph.-CH_2), 1694 (Amide-C=O), 1328 (Asymmetric), 1159 (Symmetric) (S=O); ^{1}H-NMR (DMSO-d_6, TMS, 400 MHz, δ ppm): 10.06 (1H, s, -CONH), 7.75-7.82 (4H, m, J=8, -Ar-H), 7.26 (2H, s, SO_2NH_2), 2.40 -2.54 (8H, m, N-CH_2-*CH*$_2$-N), 3.24-3.29 (1H, q, CH_3-*CH*-N); 2.28-2.33 (2H, q, CH_3-*CH*$_2$-N); 1.17-1.18 (3H, d, *J*=4 Hz C*H*$_3$-CH); 0.96-0.99 (3H, t, *J*=4 Hz *CH*$_3$-CH_2-N); ^{13}C-NMR (DMSO-d_6, TMS, 100 MHz, δ ppm): 172.37 (C=O), 142.02 (Ar-*C*-NH-), 138.87 (Ar-*C*-SO_2NH_2), 127.06 (Arom.), 119.40 (Arom.), 64.04 (CH_3-*C*H-N), 53.02 (*C*H_2-N(CH_2CH_3)-*C*H_2), 52.04 (*C*H_2-N($CHCH_3$)- *C*H_2), 49.50 (CH_3-*CH*$_2$-N); 12.92 (-CH-*C*H_3); 12.49 (*CH*$_3$-CH_2-N); LC-MS/MS Mass (*m/z*): 341.10 [M+H]; Calculated. for $C_{15}H_{24}N_4O_3S$ (340,44 g/mol) (%): C, 52.92; H, 7.11; N, 16.46; S, 9.42. Found (%): C, 52.83; H, 7.17; N, 16.57; S, 9.38.

Conclusion

Novel N^4-substituted aminobenzenesulfonamides derivatives were synthesized and subsequently studied for spectroscopic and potential biological activities. Fluorescence studies showed the derivatives as having greater intensities and efficiencies than that of precursor **1**. Physicochemical data were collected and discussed, and correlated with the observed *in vitro* cytotoxicity activities. The lipophilicities and polarities of the synthesized compounds were evaluated, and synergistic effects optimally controlling cytotoxicity activities were noted, such that, high lipophilicity and low polarity combinations were not a preferred combination, as for derivative **5**. High lipophilicities and high polarities, worked in a synergistic manner to offer both hydrogen bonding and electrostatic capabilites for cancer cell targets, as for observed for derivatives **7** and **8**. Lower lipophilicities and high polarities, though gave unremarkable activities, were an undesired combination, targeting normal cells as observed for derivative **6**. The results of the synthesized derivatives may be used to further develop carbonic anhydrase inhibitory drugs. The photophysical data may offer potential use in the analytical techniques of medicine.

Acknowledgements

Authors wish to thank Harran University (Project No. HUBAK 12059 and 12167) and the Scientific and Technological Research Council of Turkey (TUBITAK, Project No. 115Z681) and Gaziantep University (Project No. GÜ FEF.11.07) for the financial support.

Conflict of interest

The authors declare that they have no conflict of interest.

References

1 McCarthy J M, Richard G, Huck W, Tucker R M, Tosiello R L, Shan M, Heyd A & Echols R M, *Am J Med*, 106 (1999) 292.
2 Franks P & Gleiner J A, *J Fam Pract*, 19 (1984) 185.
3 Kurzer E & Kaplan S A, *Eur Urol*, 42 (2002) 163.
4 Siddiqui N, Arshad, M F, Khan S A & Ahsan W, *J Enzyme Inhib Med*, 25(4) (2010) 485.
5 Hosseinzadeh N, Seraj S, Bakhshi-Dezffoli M E, Hasani M, Khoshneviszadeh M, Fallah-Bonekohal S, Abdollahi M, Foroumadi A & Shafiee A, *Iran J Pharm Res*, 12(2) (2013) 325.
6 Ma T, Fuld A D, Rigas J R, Hagey A E, Gordon G B, Dmitrovsky E & Dragnev K H, *Chemotherapy*, 58(4) (2012) 321.
7 Bryant B & Knights K, *Pharmacology for Health Professionals*, 3rd edn. (Mosby, Australia, Elsevier) (2010).
8 Luo Y, Zhou Y, Song Y, Chen G, Wang Y X, Tian Y, Fan W W, Yang Y S, Cheng T & Zhu H L, *Bioorg Med Chem Lett*, 28(23-24), (2018) 3634.
9 Durgun M, Turkmen H, Zengin G, Zengin H, Koyunsever M & Koyuncu I, *Bioorg Chem*, 70 (2017) 163.
10 Kachaeva M V, Hodyna D M, Semenyuta I V, Pilyo S G, Prokopenko V M, Kovalishyn V V, Metelytsia L O & Brovarets V S, *Comput Bıol Chem*, 74 (2018) 294.
11 Winum J Y, Rami M, Scozzafava A, Montero J L & Supuran C, *Med Res Rev*, 28 (2008) 445.
12 Neri D & Supuran C T, *Nat Rev Drug Discov*, 10 (2011) 767.
13 Mosmann T, *J Immunol Methods*, 65(1-2) (1983) 55.
14 McDonald C P, Winum J Y, Supuran C T & Dedhar S, *Oncotarget*, 3 (2012) 84.
15 Gatenby R A & Gillies R J, *Nature Rev Cancer*, 4 (2004) 891.
16 *Practical Fluorescence*, edited by Guilbault G G (Marcel Dekker, New York, USA) (1990).
17 Gilbert A & Bagott J, *Essentials of Molecular Photochemistry* (CRC Press, Boca Raton, Florida, USA) (1991).
18 Osaheni J A & Jenekhe S A, *J Am Chem Soc*, 117(7) (1995) 7389.
19 HyperChem 7.5 Program, Hypercube Inc., Toronto, Canada, (2002).
20 Hansch C, *Accts Chem Res*, 2(8) (1969) 232.
21 Hansch C, Leo A & Hoekman D H, *Exploring QSAR. Fundamentals and Application in Chemistry and Biology* (American Chemical Society, Washington, DC, USA) (1995).
22 Leo A, Hansch C & Elkins D, *Chem Rev*, 71(6) (1971) 525.
23 *Absorption Spectra in the Ultraviolet and Visible Region*, edited by Lang L (Academic Press, New York, NY, USA) (1961).
24 Doub L & Vandenbelt J M, *J Am Chem Soc*, 71(7) (1949) 2414.
25 Zhang X, Lin Y, Liu L & Lin C, *Luminescence*, 303 (2015) 269.
26 Turkmen H, Durgun M, Yilmaztekin S, Emul M, Innocenti A, Vullo D, Scozzafava A & Supuran C T, *Bioorg Med Chem Lett*, 15(2) (2005) 367.